Science Advances

AAAS

advances.sciencemag.org/cgi/content/full/4/5/eaap8802/DC1

Supplementary Materials for

Spin- and valley-polarized one-way Klein tunneling in photonic topological insulators

Xiang Ni, David Purtseladze, Daria A. Smirnova, Alexey Slobozhanyuk, Andrea Alù, Alexander B. Khanikaev

Published 11 May 2018, *Sci. Adv.* **4**, eaap8802 (2018)
DOI: 10.1126/sciadv.aap8802

This PDF file includes:

section Sl. Low-energy effective Hamiltonians

A. Nonreciprocal crystal

In this section, we derive the effective Hamiltonian in the vicinity of Dirac points for a 2D honeycomb photonic crystal made of gyromagnetic cylinders by using the plane wave expansion method [5,12,25]. Assuming the harmonic time dependence $\sim \exp(i\omega t)$, we start with Maxwell's equations,

$$\begin{aligned} \nabla \times \mathbf{E} &= -ik_0 \hat{\mu} \mathbf{H}, \\ \nabla \times \mathbf{H} &= ik_0 \varepsilon \mathbf{E} \end{aligned} \tag{S1}$$

where $k_0 = \omega/c$ is the wavenumber in free space, ω is the angular frequency, and c is the speed of light. Material response is described by a scalar permittivity ε and the permeability tensor containing off-diagonal imaginary components

$$\hat{\mu} = \begin{pmatrix} \mu_\perp & i\varkappa & 0 \\ -i\varkappa & \mu_\perp & 0 \\ 0 & 0 & \mu_{zz} \end{pmatrix} \tag{S2}$$

Assuming the case of in-plane propagation, i.e. $\dfrac{\partial}{\partial z} = 0$, from Eq. (S1) we obtain the governing equation for the $E_z(x,y)$ electric field component of TM polarization

$$\left(k_0^2 \varepsilon + \frac{\partial}{\partial x} m \frac{\partial}{\partial x} + \frac{\partial}{\partial y} m \frac{\partial}{\partial y} \right) E_z = i \left(\frac{\partial}{\partial x} \Delta \frac{\partial}{\partial x} - \frac{\partial}{\partial y} \Delta \frac{\partial}{\partial y} \right) E_z \tag{S3}$$

where we introduced compact notations $m = \dfrac{\mu_\perp}{\mu_\perp^2 - \varkappa^2}$ and $\Delta = \dfrac{\varkappa}{\mu_\perp^2 - \varkappa^2}$. Here, we assume in-plane propagation and the permittivity perturbed by a weak periodic modulation $\varepsilon = 1 + \tilde{\varepsilon}$. Given the crystal periodicity, we apply Bloch theorem and expand the field E_z and the constitutive parameters in Fourier series as follows,

$$E_z = \sum_G E_{\mathbf{G}} \, e^{i(\mathbf{G}+\mathbf{q})\cdot\mathbf{r}} \tag{S4}$$

$$\{\tilde{\varepsilon}, m, \Delta\} = \sum_G \{\tilde{\varepsilon}_{\mathbf{G}}, m_{\mathbf{G}}, \Delta_{\mathbf{G}}\} \, e^{i\mathbf{G}\cdot\mathbf{r}} \tag{S5}$$

where $\mathbf{G}$ and $\mathbf{G}'$ denote reciprocal lattice vectors. The length of all reciprocal lattice vectors $\mathbf{G}_i$ is equal to $G = 4\pi/(\sqrt{3}a)$, where a is a lattice constant of the crystal. Substituting Eqs. (S19), (S20) into Eq. (S3), we get a set of linear equations for the Fourier components of the field

$$k_0^2 E_{\mathbf{G}} + k_0^2 \sum_{G'} \tilde{\varepsilon}_{\mathbf{G}-\mathbf{G}'} E_{\mathbf{G}'} - \sum_{G'} m_{\mathbf{G}-\mathbf{G}'} (\mathbf{q}+\mathbf{G}) \cdot (\mathbf{q}+\mathbf{G}') E_{\mathbf{G}'} = -i \sum_{G'} \Delta_{\mathbf{G}-\mathbf{G}'} \left[(q_x + G_x)(q_y + G'_y) - (q_x + G'_x)(q_y + G_y) \right] E_{\mathbf{G}'} \tag{S6}$$

We are now interested in dispersion of the modes near the K (K′) points being the corners of the crystal Brillouin zone, which correspond to the Bloch wavevectors $\mathbf{K}_\pm = K(\pm 1, 0, 0)$, where $K = \dfrac{4}{3}\dfrac{\pi}{a}$, so that for the K (K′) valleys $\mathbf{q} + \mathbf{G} = \mathbf{K}_\pm + \delta\mathbf{k} + \mathbf{G} \equiv \mathbf{k} + \delta\mathbf{k}$, where $\delta\mathbf{k}$ is a small detuning. We truncate the basis to the first three plane waves with the wavevectors $\mathbf{k}_{1,2,3} = \mathbf{K}_\pm + \mathbf{G}_{0,1,2}$ each rotated by $2\pi/3$ with respect to one another and corresponding to the reciprocal lattice vectors $\mathbf{G}_0 = (0,0)$, $\mathbf{G}_1 = K\left(\mp\dfrac{3}{2}, -\dfrac{\sqrt{3}}{2} \right)$, $\mathbf{G}_2 = K\left(\mp\dfrac{3}{2}, \dfrac{\sqrt{3}}{2} \right)$. Thus, to describe the formation of the bands, we leave only the leading contributions from three Γ points nearest to K (K′) with $\mathbf{k}_1 = (\pm K, 0)$, $\mathbf{k}_2 = K\left(\mp\dfrac{1}{2}, -\dfrac{\sqrt{3}}{2} \right)$, $\mathbf{k}_3 = K\left(\mp\dfrac{1}{2}, \dfrac{\sqrt{3}}{2} \right)$. Next, we

apply $k\cdot p$ approximation, keeping only the first order in $\delta\mathbf{k}$, $(\mathbf{k}_i+\delta\mathbf{k})\cdot(\mathbf{k}_j+\delta\mathbf{k})\approx\mathbf{k}_i\cdot\mathbf{k}_j+\delta\mathbf{k}\cdot(\mathbf{k}_i+\mathbf{k}_j)$. Neglecting the terms of higher orders of smallness, we obtain a set of three equations, which can be written in matrix form as

$$\left[k_0^2\begin{pmatrix}1+\tilde{\varepsilon}_0 & \tilde{\varepsilon}_{01} & \tilde{\varepsilon}_{02}\\ \tilde{\varepsilon}_{01}^* & 1+\tilde{\varepsilon}_0 & \tilde{\varepsilon}_{12}\\ \tilde{\varepsilon}_{02}^* & \tilde{\varepsilon}_{12}^* & 1+\tilde{\varepsilon}_0\end{pmatrix}-\begin{pmatrix}m_0\mathbf{k}_1^2 & m_{01}(\mathbf{k}_1\cdot\mathbf{k}_2) & m_{02}(\mathbf{k}_1\cdot\mathbf{k}_3)\\ m_{01}^*(\mathbf{k}_1\cdot\mathbf{k}_2) & m_0\mathbf{k}_2^2 & m_{12}(\mathbf{k}_2\cdot\mathbf{k}_3)\\ m*_{02}(\mathbf{k}_1\cdot\mathbf{k}_3) & m_{12}^*(\mathbf{k}_2\cdot\mathbf{k}_3) & m_0\mathbf{k}_3^2\end{pmatrix}\right.$$
$$\left.-\delta\mathbf{k}\cdot\begin{pmatrix}2\mathbf{k}_1m_0 & (\mathbf{k}_1+\mathbf{k}_2)m_{01} & (\mathbf{k}_1+\mathbf{k}_3)m_{02}\\ (\mathbf{k}_1+\mathbf{k}_2)m_{01}^* & 2\mathbf{k}_2m_0 & (\mathbf{k}_2+\mathbf{k}_3)m_{12}\\ (\mathbf{k}_1+\mathbf{k}_3)m_{02}^* & (\mathbf{k}_2+\mathbf{k}_3)m_{12}^* & 2\mathbf{k}_3m_0\end{pmatrix}+i\begin{pmatrix}0 & [\mathbf{k}_1\times\mathbf{k}_2]_z\Delta_{01} & [\mathbf{k}_1\times\mathbf{k}_3]_z\Delta_{02}\\ [\mathbf{k}_1\times\mathbf{k}_2]_z\Delta_{01}^* & 0 & [\mathbf{k}_2\times\mathbf{k}_3]_z\Delta_{12}\\ [\mathbf{k}_1\times\mathbf{k}_3]_z\Delta_{02}^* & [\mathbf{k}_2\times\mathbf{k}_3]_z\Delta_{12}^* & 0\end{pmatrix}\right]\begin{pmatrix}E_{\mathbf{G}_0}\\ E_{\mathbf{G}_1}\\ E_{\mathbf{G}_2}\end{pmatrix}=0$$

The Fourier coefficients comprising the above system are defined as

$$\{\tilde{\varepsilon},m,\Delta\}_{ij}=\frac{1}{S_0}\int\limits_{\text{u.c.}}\{\tilde{\varepsilon},m,\Delta\}(x,y)\,e^{-i(\mathbf{G}_i-\mathbf{G}_j)\cdot\mathbf{r}}\,d^2\mathbf{r}_\perp \tag{S7}$$

where $S_0=a^2\sqrt{3}/2$ is the area of the structure unit cell, and the index $(\mathbf{G}_i-\mathbf{G}_j)\equiv\mathbf{G}_{ij}$ is abbreviated as ij. In particular, coefficients $\{\tilde{\varepsilon},m,\Delta\}_{00,11,22}\equiv\{\tilde{\varepsilon},m,\Delta\}_0$ imply averaged over the unit cell spatial distributions. Additionally, we make use of a honeycomb symmetry of the lattice. To take into account a slight difference of two rods A and B in the unit cell, we write

$$\{\tilde{\varepsilon},m,\Delta\}(\mathbf{r}_\perp)=\left(\left\{\bar{\tilde{\varepsilon}},\bar{m},\bar{\Delta}\right\}-\frac{1}{2}\delta\{\tilde{\varepsilon},m,\Delta\}\right)\Pi(\mathbf{r}_\perp-\mathbf{v}_1)+\left(\left\{\bar{\tilde{\varepsilon}},\bar{m},\bar{\Delta}\right\}+\frac{1}{2}\delta\{\tilde{\varepsilon},m,\Delta\}\right)\Pi(\mathbf{r}_\perp+\mathbf{v}_1) \tag{S8}$$

where $\mathbf{v}_1=-\mathbf{r}_{\text{AB}}/2$, $\mathbf{r}_{\text{AB}}$ denotes the vector pointing from A to B, and step functions $\Pi(\mathbf{r}_\perp\pm\mathbf{v}_1)$ are localized on the lattice sites. Thereby, coefficients (S7) take the form

$$\{\tilde{\varepsilon},m,\Delta\}_{ij}=\frac{I_1}{S_0}\left(\left\{\bar{\tilde{\varepsilon}},\bar{m},\bar{\Delta}\right\}2\cos\varphi_{ij}+i\delta\{\tilde{\varepsilon},m,\Delta\}\sin\varphi_{ij}\right)\equiv\{\tilde{\varepsilon},m,\Delta\}_1\,2\cos\varphi_{ij}+i\delta\{\tilde{\varepsilon},m,\Delta\}_{\text{AB}}\sin\varphi_{ij} \tag{S9}$$

where $\varphi_{ij}=(\mathbf{G}_{ij}\cdot\mathbf{v}_1)$. Choosing $\mathbf{v}_1=(0,1)\,\dfrac{d}{2}$, where $d=\dfrac{a}{\sqrt{3}}$ is a distance between cylinders A and B , we calculate the angles $\varphi_{01}=-\varphi_{02}=\varphi_{20}=-\varphi_{10}=\pi/3$, $\varphi_{12}=-2\pi/3=-\varphi_{21}$. Finally, in the case of codirectional magnetization, we reach a set of equations

$$k_0^2(1+\hat{\varepsilon})\mathscr{E}=\left(\hat{m}+\hat{m}_{AB}+\hat{\theta}_{\text{g}}\right)\mathscr{E} \tag{S10}$$

where the column-vector $\mathscr{E}=(E_{\mathbf{G}_0},E_{\mathbf{G}_1},E_{\mathbf{G}_2})^{\text{T}}$, and 3×3 matrices are given by

$$\hat{m}=K^2\begin{pmatrix}m_0 & -\frac{1}{2}m_1 & -\frac{1}{2}m_1\\ -\frac{1}{2}m_1 & m_0 & \frac{1}{2}m_1\\ -\frac{1}{2}m_1 & \frac{1}{2}m_1 & m_0\end{pmatrix}\pm K\delta k_x\begin{pmatrix}2m_0 & \frac{1}{2}m_1 & \frac{1}{2}m_1\\ \frac{1}{2}m_1 & -m_0 & m_1\\ \frac{1}{2}m_1 & m_1 & -m_0\end{pmatrix}+K\delta k_y\begin{pmatrix}0 & -\frac{\sqrt{3}}{2}m_1 & \frac{\sqrt{3}}{2}m_1\\ -\frac{\sqrt{3}}{2}m_1 & -\sqrt{3}m_0 & 0\\ \frac{\sqrt{3}}{2}m_1 & 0 & \sqrt{3}m_0\end{pmatrix},$$

$$\hat{m}_{AB}=i\delta m_{\text{AB}}K^2\left(-\frac{1}{2}\right)\begin{pmatrix}0 & \frac{\sqrt{3}}{2} & -\frac{\sqrt{3}}{2}\\ -\frac{\sqrt{3}}{2} & 0 & -\frac{\sqrt{3}}{2}\\ \frac{\sqrt{3}}{2} & \frac{\sqrt{3}}{2} & 0\end{pmatrix},\quad \hat{\theta}_{\text{g}}=\mp i\Delta_1K^2\begin{pmatrix}0 & -\frac{\sqrt{3}}{2} & \frac{\sqrt{3}}{2}\\ \frac{\sqrt{3}}{2} & 0 & \frac{\sqrt{3}}{2}\\ -\frac{\sqrt{3}}{2} & -\frac{\sqrt{3}}{2} & 0\end{pmatrix},\quad \hat{\varepsilon}=\begin{pmatrix}\tilde{\varepsilon}_0 & \tilde{\varepsilon}_1 & \tilde{\varepsilon}_1\\ \tilde{\varepsilon}_1 & \tilde{\varepsilon}_0 & -\tilde{\varepsilon}_1\\ \tilde{\varepsilon}_1 & -\tilde{\varepsilon}_1 & \tilde{\varepsilon}_0\end{pmatrix}$$

Thus, we obtain 3×3 eigenvalue problem, $k_0^2\mathscr{E}=(1+\hat{\varepsilon})^{-1}\left(\hat{m}+\hat{m}_{AB}+\hat{\theta}_{\text{g}}\right)\mathscr{E}=\hat{H}_1\mathscr{E}$.
As the next step we perform a unitary transformation $\hat{H}=U\hat{H}_1U^{-1}$ with the matrix

$$U=\frac{1}{\sqrt{3}}\begin{pmatrix}e^{2i\pi/3} & e^{-i\pi/3} & -1\\ 1 & e^{-i\pi/3} & e^{i\pi/3}\\ e^{i\pi/3} & e^{-2i\pi/3} & e^{-2i\pi/3}\end{pmatrix} \tag{S11}$$

We note that the third row of the transformed effective Hamiltonian describes a nondegenerate singlet TM state which is separated from the doublet state by the energy gap $\approx3\times m_1$, and therefore, in accord with the perturbation theory, its mixing with the

doublet states is strongly suppressed. As the result, this state can be eliminated from the effective Hamiltonian. We note that numerical simulations confirm that such singlet state is always separated from the doublet by a complete photonic band gap. Thus, we recover the following effective massive Dirac Hamiltonian in the subspace of the doublet states after anticlockwise rotating the vector $(\delta k_x, \delta k_y)$ by $\frac{4\pi}{3}$,

$$\hat{H}_{\mathrm{K}(\mathrm{K}')} = \Omega_0 \pm V\delta k_x \hat{\sigma}_x + V\delta k_y \hat{\sigma}_y + (\pm m_{\mathrm{T}} - m_{\mathrm{I}})\hat{\sigma}_z \tag{S12}$$

where the unperturbed frequency $\Omega_0 = \dfrac{K^2\left(m_0 - \dfrac{1}{2}m_1\right)}{1+\tilde{\varepsilon}_0+\tilde{\varepsilon}_1}$, velocity $V = \dfrac{K(m_0+m_1)}{1+\tilde{\varepsilon}_0+\tilde{\varepsilon}_1}$, and mass terms due to parity breaking $m_{\mathrm{I}} = -\dfrac{3K^2\delta m_{\mathrm{AB}}}{4(1+\tilde{\varepsilon}_0+\tilde{\varepsilon}_1)}$, and time-reversal symmetry breaking $m_{\mathrm{T}} = \dfrac{3K^2\Delta_1}{2(1+\tilde{\varepsilon}_0+\tilde{\varepsilon}_1)}$.

For the case of oppositely magnetized cylinders, in place of imaginary matrices $\hat{m}_{AB}$ and $\hat{\theta}$, we have a real matrix

$$M = \frac{3}{4}K^2\delta\Delta_{\mathrm{AB}}\begin{pmatrix} 0 & \pm 1 & \pm 1 \\ \pm 1 & 0 & \mp 1 \\ \pm 1 & \mp 1 & 0 \end{pmatrix} \tag{S13}$$

leading to the Dirac Hamiltonians

$$\hat{H}_{\mathrm{K}(\mathrm{K}')} = \Omega_0 \pm \delta\Omega_0 \pm V\delta k_x \hat{\sigma}_x + V\delta k_y \hat{\sigma}_y \tag{S14}$$

with opposite frequency detunings $\delta\Omega_0 = \dfrac{3}{4}K^2\delta\Delta_{\mathrm{AB}}$ in different valleys.

B. Bianisotropic crystal

In this section we derive the effective Hamiltonian near the Dirac points for a triangular lattice of deformed (triangulated) rods made of a bianisotropic material. Similar to Sec. A, we start with Maxwell's equations

$$\begin{aligned} \nabla\times\mathbf{E} &= -ik_0(\hat{\mu}\mathbf{H} + \hat{\chi}\mathbf{E}), \\ \nabla\times\mathbf{H} &= ik_0(\hat{\varepsilon}\mathbf{E} + \hat{\chi}^{\dagger}\mathbf{H}) \end{aligned} \tag{S15}$$

with the constitutive tensors defined as follows

$$\hat{\varepsilon} = \begin{pmatrix} \varepsilon_\perp & 0 & 0 \\ 0 & \varepsilon_\perp & 0 \\ 0 & 0 & \varepsilon_{zz} \end{pmatrix}, \quad \hat{\mu} = \begin{pmatrix} \mu_\perp & 0 & 0 \\ 0 & \mu_\perp & 0 \\ 0 & 0 & \mu_{zz} \end{pmatrix}, \quad \hat{\chi} = \begin{pmatrix} 0 & i\chi & 0 \\ -i\chi & 0 & 0 \\ 0 & 0 & 0 \end{pmatrix} \tag{S16}$$

where we assume $\hat{\varepsilon} = \hat{\mu}$ and χ are purely real. From Eq. (S15), one can recover a reduced set of equations for TM-like and TE-like modes coupled to each other by bianisotropy

$$\left(k_0^2\varepsilon_{zz} + \partial_x \mathrm{e}\partial_x + \partial_y \mathrm{e}\partial_y\right)E_z = -i\left(\partial_x\Delta\partial_y + \partial_y\Delta\partial_x\right)H_z, \tag{S17a}$$

$$\left(k_0^2\mu_{zz} + \partial_x m\partial_x + \partial_y m\partial_y\right)H_z = -i\left(\partial_x\Delta\partial_y + \partial_y\Delta\partial_x\right)E_z \tag{S17b}$$

where we use the following denotations $m = \dfrac{\mu_\perp}{\mu_\perp\varepsilon_\perp - \chi^2}$, $\mathrm{e} = \dfrac{\varepsilon_\perp}{\mu_\perp\varepsilon_\perp - \chi^2}$, and $\Delta = \dfrac{\chi}{\mu_\perp\varepsilon_\perp - \chi^2}$. Combining equations (S17) and taking into account equality $\mathrm{e} = m$, we find that two polarizations (spins), defined as $\psi^{\uparrow,\downarrow} = E_z \pm H_z$, satisfy uncoupled equations, analogous to Eq. (S3),

$$\left(k_0^2\varepsilon_{zz} + \partial_x m\partial_x + \partial_y m\partial_y\right)\psi^{\uparrow,\downarrow} = \mp i\left(\partial_x\Delta\partial_y + \partial_y\Delta\partial_x\right)\psi^{\uparrow,\downarrow} \tag{S18}$$

For simplicity, we set $\varepsilon_{zz} = \varepsilon = \mathrm{const}$ in Eq. (S18) and apply the plane-wave expansion method, following the procedure described in Sec. I. Considering the spin up, we apply Bloch theorem and expand the field $\psi^{\uparrow}$ and the constitutive parameters in Fourier series,

$$\psi^{\uparrow} = \sum_G \psi^{\uparrow}_{\mathbf{G}} e^{i(\mathbf{G}+\mathbf{q})\cdot\mathbf{r}} \tag{S19}$$

$$\{m, \Delta\} = \sum_G \{m_{\mathbf{G}}, \Delta_{\mathbf{G}}\}\, e^{i\mathbf{G}\cdot\mathbf{r}} \tag{S20}$$

where the Fourier coefficients are given by

$$\{m,\Delta\}_{ij} = \frac{1}{S_0}\int\limits_{\text{u.c.}} \{\tilde{\varepsilon},m,\Delta\}(x,y)\, e^{-i(\mathbf{G}_i-\mathbf{G}_j)\cdot\mathbf{r}}\, d^2\mathbf{r}_\perp \tag{S21}$$

where we keep to the notations of Sec. A. Substituting Eqs. (S19), (S20) into Eq. (S18), we get a set of linear equations for the Fourier components of the field

$$k_0^2\varepsilon\psi^{\uparrow}_{\mathbf{G}} - \sum_{G'} m_{\mathbf{G}-\mathbf{G}'}(\mathbf{q}+\mathbf{G})\cdot(\mathbf{q}+\mathbf{G}')\psi^{\uparrow}_{\mathbf{G}'} = i\sum_{G'}\Delta_{\mathbf{G}-\mathbf{G}'}\left[(q_x+G_x)(q_y+G'_y)-(q_x+G'_x)(q_y+G_y)\right]\psi^{\uparrow}_{\mathbf{G}'} \tag{S22}$$

Adopting $k\cdot p$ approximation, we restrict to the linear order near K point. Due to C_{3v} rotational symmetry, $\Delta_{01}=\Delta_{02}=\Delta_{12}=\Delta_1$. To account for triangulation, we introduce three small circular perturbations of radius r_2 attached to the unperturbed circular rod of radius r_1, whose centers locations are determined by the vectors $\mathbf{d}_1 = d_0\left(-\frac{\sqrt{3}}{2},-\frac{1}{2}\right)||\mathbf{G}_{10}$, $\mathbf{d}_2 = d_0(0,1)||\mathbf{G}_{21}$, $\mathbf{d}_3 = d_0\left(\frac{\sqrt{3}}{2},-\frac{1}{2}\right)||\mathbf{G}_{02}$, where $d_0 = r_1+r_2$. Accordingly, we write the spatial distribution as

$$m(\mathbf{r}_\perp) = m_{\text{env}} + (m_{\text{rod}}-m_{\text{env}})\left(\Pi(\mathbf{r}_\perp,r_1)+\sum_{n=1}^{3}\Pi(\mathbf{r}_\perp-\mathbf{d}_n,r_2)\right) \tag{S23}$$

where function $\Pi(\mathbf{r}_\perp,r_{1,2})$ are rectangular functions of the widths $2r_{1,2}$, values m_{env} and m_{rod} correspond to the environment and interior of cylinders. Thereby, the Fourier coefficients m_{ij} can be written as

$$m_{ij} = \begin{cases} m_0+3\Delta m_0(r_2), & i=j \\ m_1+\Delta m_1(r_2)\sum\limits_{n=1}^{3} e^{-i(\mathbf{G}_i-\mathbf{G}_j)\mathbf{d}_n}, & i\neq j \end{cases} \tag{S24}$$

We obtain 3×3 eigenvalue problem,

$$k_0^2\varepsilon\vec{\psi}^{\uparrow} = \left(\hat{m}+\hat{m}_{\text{tri}}+\hat{\theta}_{\text{b}}\right)\vec{\psi}^{\uparrow} \tag{S25}$$

where the column-vector $\vec{\psi}^{\uparrow} = (\psi^{\uparrow}_{\mathbf{G}_0},\psi^{\uparrow}_{\mathbf{G}_1},\psi^{\uparrow}_{\mathbf{G}_2})^{\text{T}}$, and 3×3 matrices are given by

$$\hat{m} = K^2\begin{pmatrix} m_0 & -\frac{1}{2}m_1 & -\frac{1}{2}m_1 \\ -\frac{1}{2}m_1 & m_0 & -\frac{1}{2}m_1 \\ -\frac{1}{2}m_1 & -\frac{1}{2}m_1 & m_0 \end{pmatrix} + K\delta k_x\begin{pmatrix} 2m_0 & \frac{1}{2}m_1 & \frac{1}{2}m_1 \\ \frac{1}{2}m_1 & -m_0 & -m_1 \\ \frac{1}{2}m_1 & -m_1 & -m_0 \end{pmatrix} + K\delta k_y\begin{pmatrix} 0 & -\frac{\sqrt{3}}{2}m_1 & \frac{\sqrt{3}}{2}m_1 \\ -\frac{\sqrt{3}}{2}m_1 & -\sqrt{3}m_0 & 0 \\ \frac{\sqrt{3}}{2}m_1 & 0 & \sqrt{3}m_0 \end{pmatrix},$$

$$\hat{m}_{\text{tri}} = iK^2\begin{pmatrix} 3\Delta m_0 & -\frac{1}{2}\Delta m_1\left(e^{i\varphi}+2e^{-i\varphi/2}\right) & -\frac{1}{2}\Delta m_1\left(e^{-i\varphi}+2e^{i\varphi/2}\right) \\ -\frac{1}{2}\Delta m_1\left(e^{-i\varphi}+2e^{i\varphi/2}\right) & 3\Delta m_0 & -\frac{1}{2}\Delta m_1\left(e^{i\varphi}+2e^{-i\varphi/2}\right) \\ -\frac{1}{2}\Delta m_1\left(e^{i\varphi}+2e^{-i\varphi/2}\right) & -\frac{1}{2}\Delta m_1\left(e^{-i\varphi}+2e^{i\varphi/2}\right) & 3\Delta m_0 \end{pmatrix},$$

$$\hat{\theta}_{\text{b}} = i\Delta_1K^2\frac{\sqrt{3}}{2}\begin{pmatrix} 0 & -1 & 1 \\ 1 & 0 & -1 \\ -1 & 1 & 0 \end{pmatrix}$$

where $\varphi = \sqrt{3}Kd_0$.
To change the basis, we perform the unitary transformation $\hat{H} = U\hat{H}_1U^{-1}$ with the matrix

$$U = \frac{1}{\sqrt{3}}\begin{pmatrix} 1 & 1 & 1 \\ 1 & e^{-2i\pi/3} & e^{2i\pi/3} \\ 1 & e^{2i\pi/3} & e^{-2i\pi/3} \end{pmatrix} \tag{S26}$$

After excluding the first row describing a singlet state, we get the effective 2×2 Hamiltonian in the subspace of the doublet states. The same procedure can be repeated for the opposite valley and spin. Finally, we arrive at the Hamiltonian for two spin configurations

$$H^{\uparrow,\downarrow}=\begin{pmatrix}(\Omega_0+\Delta\Omega_0)\hat{\sigma}_0+V(\delta k_x\hat{\sigma}_x+\delta k_y\hat{\sigma}_y)+[m_{\rm I}\pm m_{\rm B}]\hat{\sigma}_z & 0\\ 0 & (\Omega_0+\Delta\Omega_0)\hat{\sigma}_0+V(-\delta k_x\hat{\sigma}_x+\delta k_y\hat{\sigma}_y)+[m_{\rm I}\mp m_{\rm B}]\hat{\sigma}_z,\end{pmatrix} \tag{S27}$$

where the unperturbed frequency $\Omega_0=K^2\left(m_0+\frac{1}{2}m_1\right)$, $\Delta\Omega_0=K^2\left(3\Delta m_0+\Delta m_1\cos\frac{\varphi}{2}+\Delta m_1\frac{1}{2}\cos\varphi\right)$, velocity $V=K(m_0-m_1)$, and mass terms due to inversion symmetry breaking $m_{\rm I}=K^2\sqrt{3}\Delta m_1\sin\frac{\varphi}{2}\left(\cos\frac{\varphi}{2}-1\right)$, and bianisotropy $m_{\rm B}=\frac{3}{2}K^2\Delta_1$.

section S2. Nonreciprocal tunneling in photonic graphene with a single potential barrier

In this section, we provide a derivation of Eq. (3) of the main text. Geometry sequence of the structure we consider is $1/2/1$, where domains 1 and 2 are characterized by total masses $m_{1,2}$ and potentials $u_{1,2}$, and these masses arise from the symmetry breaking of the lattice and can be expressed in terms of material parameters such as permittivity ε and permeability μ. $u_{1,2}$ are the effective photonic potentials for domain 1 and domain 2, respectively. The wave excited with the angular frequency $\Omega((\Omega-\Omega_0-u_1)^2>m_1^2)$ is propagating from the region 1 along the x axis onto the potential obstacle of the amplitude (u_2-u_1) in the domain 2, which is infinitely long in y direction and has a finite width L in x direction.
First, we solve for the wave functions in each of the regions with the effective Hamiltonian in domains 1 at valley K adopted from Eq. (S14) and in domain 2 from Eq. (S12). For definiteness, we consider the case of a nonreciprocal crystal here, the same method can be applied in the case of a bianisotropic crystal. The inter-valley scattering can be ignored, if the potential barrier is relatively small and smooth. Thereby, the two-component wave function in the dipolar basis has the form $\Psi(x)=\psi(x)e^{iKx}$ with the slowly varying amplitude $\psi(x)$ expressed as

$$\begin{aligned}\psi_1(x)&=e^{i\delta k_{1x}x}\begin{pmatrix}1\\ s_1\end{pmatrix}+re^{-i\delta k_{1x}x}\begin{pmatrix}1\\ -s_1\end{pmatrix},\quad \text{if}\quad x<0,\\ \psi_2(x)&=ae^{i\delta k_{2x}x}\begin{pmatrix}1\\ s_2\end{pmatrix}+be^{-i\delta k_{2x}x}\begin{pmatrix}1\\ -s_2\end{pmatrix},\quad \text{if}\quad 0<x<L,\\ \psi_3(x)&=te^{i\delta k_{1x}x}\begin{pmatrix}1\\ s_1\end{pmatrix},\quad \text{if}\quad x>L\end{aligned} \tag{S28}$$

where $s_{1,2}=V\delta k_{1,2x}/(\Omega-\Omega_0-u_{1,2}-m_{1,2})$, and dispersion relation $(\Omega-\Omega_0-u_{1,2})^2=m_{1,2}^2+(V\delta k_{1,2x})^2$. We then apply the continuity boundary conditions at the interfaces $x=0$ and $x=L$,

$$\begin{aligned}\psi_1(x=0)&=\psi_2(x=0),\\ \psi_2(x=L)&=\psi_3(x=L)\end{aligned} \tag{S29}$$

and obtain the amplitude coefficients of the reflected and transmitted waves

$$\begin{aligned}r&=\frac{i(s_2^2-s_1^2)\sin(\delta k_{2x}L)}{2s_1s_2\cos(\delta k_{2x}L)-i(s_1^2+s_2^2)\sin(\delta k_{2x}L)},\\ t&=\frac{2s_1s_2e^{-i\delta k_{2x}L}}{2s_1s_2\cos(\delta k_{2x}L)-i(s_1^2+s_2^2)\sin(\delta k_{2x}L)}\end{aligned} \tag{S30}$$

The reflection and transmission coefficients are found from Eqs. (S30) by using definitions $R=|r|^2$, $T=1-R$, which yields Eq. (3) discussed in the main text. Note, conditions (S29) stem from the continuity of the electric field E_z tangential to the interfaces. According to Eq. (S4), this implies the continuity of the Fourier components $E_{\mathbf{G}_{0,1,2}}$. In the framework of the perturbation theory in small parameter $\kappa/\mu_\perp$, the tangential Fourier components of the magnetic field, approximated as $H_{y\mathbf{G}_{0,1,2}}\approx\frac{k_{x1,2,3}}{\mu_\perp k_0}E_{\mathbf{G}_{0,1,2}}+O(\kappa/\mu_\perp)$, are also continuous. Hence, the expression (3) adequately describes transmission of the electromagnetic waves through smoothly perturbed regions in such structured media.

Depending on relative values of Ω, u_2 and m_2, formula (3) of the main text can be split into two cases that we write out now explicitly:

$$T(\Omega) = \frac{1}{\left(1+\frac{1}{4}\sinh^2(\delta\kappa_{2x}L)\left[\frac{s_1}{c_2}+\frac{c_2}{s_1}\right]^2\right)}, \quad \text{if} \quad m_2^2 > (\Omega-u_2)^2 \tag{S31a}$$

$$T(\Omega) = \frac{1}{\left(1+\frac{1}{4}\sin^2(\delta k_{2x}L)\left[\frac{s_1}{s_2}-\frac{s_2}{s_1}\right]^2\right)}, \quad \text{if} \quad m_2^2 < (\Omega-u_2)^2 \tag{S31b}$$

where $s_1 = \sqrt{\Omega^2-m_1^2}/(\Omega-m_1)$, $c_2 = \sqrt{m_2^2-(\Omega-u_2)^2}/(\Omega-u_2-m_2)$, $s_2 = \sqrt{(\Omega-u_2)^2-m_2^2}/(\Omega-u_2-m_2)$, $\delta\kappa_{2x} = \sqrt{m_2^2-(\Omega-u_2)^2}/V$, $\delta k_{2x} = \sqrt{(\Omega-u_2)^2-m_2^2}/V$. Here, we set $\Omega_0 = u_1 = 0$ and assume $\Omega^2 > m_1^2$. In particular, (i) the trivial case $u_2 = 0$ (no barrier), and (ii) setting $m_2 = m_1 = 0$ (Klein paradox) return unity transmission.

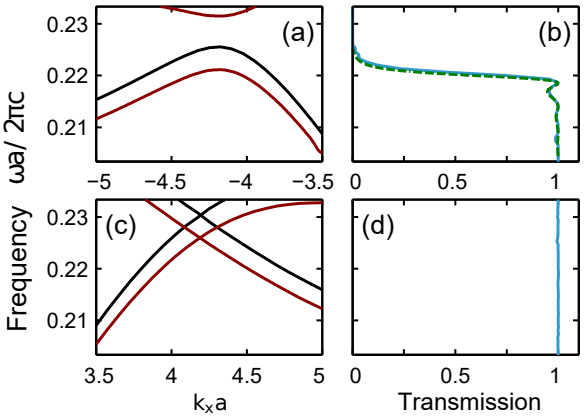

fig. S1. Photonic bands and transmission spectra. Photonic bands (a,c) and transmission coefficients (b,d) for $1/2/1$ supercell made of the gapped nonreciprocal crystals with $m_1 = m_2 = m$. Panels (a,b) and (c,d) correspond to the backward and forward wave propagation, respectively. Transmission calculated numerically is plotted with a blue line. Green dashed curve is the analytically retrieved dependence. Parameters used are the same as in the main text Fig. 2.

Figure S1 presents additional calculated results for nonreciprocal tunneling in the case where the side domains 1 and the middle domain 2 are all made of PT-violating gapped crystals.

section S3. Specific designs of spin-valle--coupled metacrystals with one-way Dirac cones

We propose a realistic design based on the meta-waveguide, which is amenable to physical implementation at microwave frequencies [24,26]. The meta-waveguide consists of two parallel metal plates, with the triangular array of compound metal rods embedded between the plates, as shown in fig. S2 (a). The parameters of the structure are adjusted in a way to resume the degeneracy between TE and TM modes. A small air gap is present between lower and upper rods to avoid the penetration of the spurious modes into the bandgap region near the Γ point. The rods attached to the bottom plate are triangulated to break the in-plane inversion symmetry, while the attached to the upper plate are shorter and are kept of the circular shape in order to break the out-of-plane inversion symmetry, thus mixing TE and TM modes. These two symmetry breaking mechanisms give rise to two distinct mass terms in the effective Hamiltonian near K (K$'$) points. Importantly, the mass terms behave in a dissimilar way for different valleys and pseudo-spin states. We tune the parameters of the structure in such a way that the mass terms cancel each other out at K$'$ (K), while they double at K (K$'$) for the pseudo-spin up (down) state.

First-principle finite element method numerical calculations are carried out to obtain the band structure, the eigenmodes, and the phase difference of their fields for the triangular array, see fig. S2 (b). The (pseudo) spin-up (spin-down) bands depicted by red (blue) lines have a bandgap at K (K$'$), while they are degenerate at K$'$ (K), and two states are mixed when they approach the Γ point, as indicated by the blurred color of the bands. One way to characterize pseudo-spin states is to evaluate the phase difference $\Delta\Phi$ between E_z and H_z field components of the modes. As shown in the left (at K$'$) and right (at K) panels of

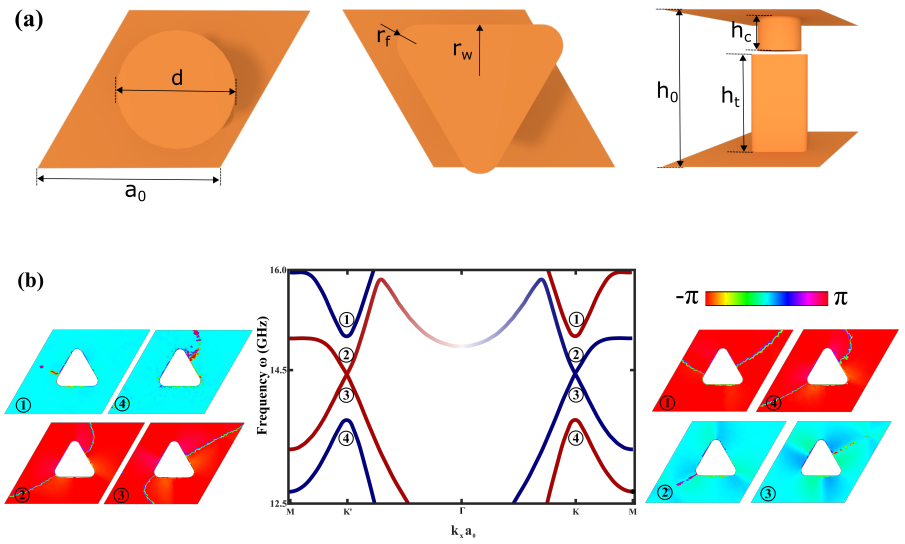

fig. S2. Schematics of the meta-waveguide design and band structures. (a) Schematics of the meta-waveguide design. From left to right: the top (circular), bottom (triangulated) parts of the structure and the side view of the unit cell, respectively. (b) Band structure for the triangular array of the rodes in the meta-waveguide (middle panel), and the phase differences between E_z and H_z for different bands (from top to bottom) at K′ (left panel) and K (right panel) points, respectively. Parameters: the lattice constant $a_0 = 16$ mm, diameter of the rod $d = 5.52$ mm, distance from the center to the side of the equilateral triangle $r_w = 2.32$ mm, with the fillet radius at each corner $r_f = 0.86$ mm, the distance between the parallel plates $h_0 = 16$ mm, and heights of the triangulated and circular rods are $h_t = 11.52$ mm and $h_c = 4$ mm, respectively.

Figure S2(b), E_z and H_z are in phase for the spin-up states, with $\Delta\Phi = 0$, while E_z and H_z appear out-of-phase for the spin-down states, with $\Delta\Phi = \pi$.